

Molecular Alignment and Orientation: From Laser-Induced Mechanisms to Optimal Control

Osman Atabek and Claude M. Dion

ABSTRACT. Genetic algorithms, as implemented in optimal control strategies, are currently successfully exploited in a wide range of problems in molecular physics. In this context, laser control of molecular alignment and orientation remains a very promising issue with challenging applications extending from chemical reactivity to nanoscale design. We emphasize the complementarity between basic quantum mechanisms monitoring alignment/orientation processes and optimal control scenarios. More explicitly, if on one hand we can help the optimal control scheme to take advantage of such mechanisms by appropriately building the targets and delineating the parameter sampling space, on the other hand we expect to learn, from optimal control results, some robust and physically sound dynamical mechanisms. One of the basic mechanisms for alignment (i.e., molecular axis parallel to field polarization) is related to the pendular states accommodated by the molecule-plus-field effective potential. The laser control of alignment can be reached by an adiabatic transport of an initial isotropic rotational state on some pendular state trapping the molecule in well-aligned geometries. Symmetry breaking mechanisms are to be looked for when orientation (i.e., molecular axis in the same direction as field polarization) is the goal of laser control. Two mechanisms are considered. The first is based upon an asymmetric pulse combining a frequency ω and its second harmonic 2ω resonant with a vibrational transition. A much more efficient mechanism is the so-called “kick” that a highly asymmetric sudden pulse can impart to the molecule. Half-cycle pulses, within the reach of current experimental technology, are among good candidates for producing such kicks. Very interestingly, an optimal control scheme for orientation, based on genetic algorithms, also leads to a sudden pulsed field bearing the characteristic features of the kick mechanism. Optimal pulse shaping for very efficient and long-lasting orientation, together with robustness with respect to temperature effects, are among our future prospects.

1. Introduction

Laser-induced molecular alignment and orientation are challenging control issues with a wide range of applications, extending from chemical reactivity to

1991 *Mathematics Subject Classification.* Primary 81V55; Secondary 35Q40.

This work benefited from the financial support of an *Action Concertée Incitative Jeunes Chercheurs* of the French Ministry of Research and from a grant of computer time from the *Institut du Développement et des Ressources Informatiques Scientifiques* of the CNRS.

nanoscale design [6, 7, 20, 24, 26, 27]. They address molecular manipulation, involving external angular degrees of freedom, aiming at a parallel positioning of the molecular axis with respect to the laser polarization vector (*alignment*) or, even more demanding, with a given direction (*orientation*). One of the basic motivations remains the drastic increase of reactive cross sections, highly sensitive to stereodynamical effects (frontal collisions). Laser-induced isomerization [10, 19], isotope separation [6], molecular trapping [23], or surface processing and catalysis [7, 24, 27] are some of the illustrations of the widely growing interest in molecular manipulation.

The most common idea is to excite a broad rotational band ΔJ in order to recover a narrow angular distribution $\Delta\theta$, through the celebrated relation $\Delta J \Delta\theta \sim \hbar$ (J being the total angular momentum and θ the molecule-laser angle). Our approach to this problem is, however, different. The emphasis is put on the depiction and study of some laser-induced dynamical mechanisms that are relevant to the alignment/orientation process: pendular states in high-frequency fields; two-photon (fundamental and second-harmonic) excitations; the kick mechanism. The question of how to take advantage of such mechanisms in a control scheme is brought up only in a second step. Adiabatic transport from an isotropic distribution to a pendular state; two IR laser pulses with frequencies in a ratio 2, the second harmonic being in resonance with a vibrational transition; very asymmetric and short-duration (sudden) half-cycle pulses imparting sudden kicks to the molecule, are some of the scenarios which are depicted and discussed in the following. Finally, in a third step, this knowledge is fully exploited in optimal control schemes, not merely for initial guesses in parameter sampling, but mainly to get a better understanding and interpretation of otherwise black-box type calculations.

The paper is organized as follows. Section 2 is devoted to intense laser alignment of the HCN molecule, through pendular states as the elementary mechanism and adiabatic/sudden transport as the control strategy. Section 3 presents the two-color orientation of HCN by a parity mixing scenario in the rotational distribution. The kick mechanism with a half-cycle pulse sudden excitation scenario is examined in section 4, as illustrated on the LiCl molecule. Sudden-excitation-based optimal control scenarios, with a thorough analysis of the role of different orientation criteria, are analyzed, using HCN and LiF, in section 5.

2. Laser-controlled alignment

2.1. The model. The linear HCN molecule, taken as an illustrative example, is described by its internal stretching motions (collectively labelled \mathbf{R}) and external rotational motions described by its polar θ and azimuthal φ angles with respect to the laser polarization vector (see figure 1). The Hamiltonian involves a single Born-Oppenheimer potential curve $V(\mathbf{R})$ (the molecular electronic ground state) and the radiative coupling $\hat{H}_{\text{rad}}(\mathbf{R}, \theta, \varphi, t)$ given by the scalar product of the field-induced dipole moment $\boldsymbol{\mu}(\mathbf{R})$ with the electric field amplitude $\mathcal{E}(t)$, i.e.,

$$(2.1) \quad \hat{H}(\mathbf{R}, \theta, \varphi, t) = \hat{T}_{\mathbf{R}} + \frac{\hbar^2}{2I(\mathbf{R})} \hat{J}^2 + V(\mathbf{R}) + \hat{H}_{\text{rad}}(\mathbf{R}, \theta, \varphi, t),$$

where $\hat{T}_{\mathbf{R}}$ is the kinetic energy operator in \mathbf{R} , \hat{J}^2 the angular momentum operator, and $I(\mathbf{R})$ the moment of inertia of the molecule. The dipole moment itself is taken

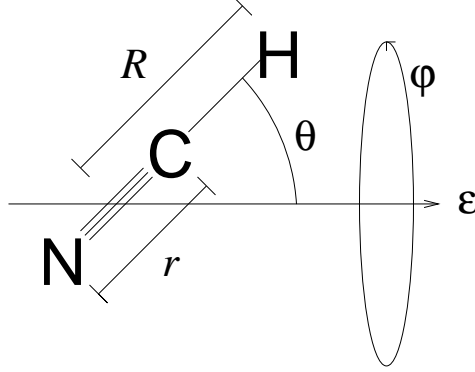


FIGURE 1. The linear HCN molecule positioned, with respect to the polarization axis \mathcal{E} of the laser, by its polar θ and azimuthal φ angles. Internal stretching coordinates are collectively noted $\mathbf{R} = (R, r)$.

as the sum of a permanent dipole μ_0 and a polarizability $\bar{\bar{\alpha}}$

$$(2.2) \quad \mu(\mathbf{R}, t) = \mu_0 + \frac{1}{2} \bar{\bar{\alpha}} \cdot \mathcal{E}(t),$$

such that

$$(2.3) \quad \hat{H}_{\text{rad}}(\mathbf{R}, \theta, \varphi, t) = -\mu_0 \mathcal{E}(t) \cos \theta - \frac{1}{2} \mathcal{E}^2(t) (\alpha_{\parallel} \cos^2 \theta + \alpha_{\perp} \sin^2 \theta).$$

In the last equation, we have made use of the fact that, for a linear molecule, $\bar{\bar{\alpha}} = \text{Diag} \{ \alpha_{xx}, \alpha_{yy}, \alpha_{zz} \}$, with $\alpha_{xx} = \alpha_{yy} \equiv \alpha_{\perp}$ and $\alpha_{zz} \equiv \alpha_{\parallel}$, when the z axis is chosen to be collinear with the molecular axis. Due to cylindrical symmetry and since the laser-molecule coupling term does not depend explicitly on φ , the motion on φ can be considered separately and is no longer taken into account.

The laser pulses are of the form $\mathcal{E}(t) = \mathcal{E}_0(t) \cos(\omega t + \phi)$, with $\mathcal{E}_0(t)$ the time varying envelope of the electric field of frequency ω and phase ϕ . We will consider laser pulses of a maximum intensity of the order of 10^{13} W/cm^2 , to avoid ionization damage to the molecule. The frequency ω is taken in the infra-red region, so it is considerably higher than the rotational frequency of the molecule.

The dynamics of the molecular system are then obtained by solving numerically the time-dependent Schrödinger equation

$$(2.4) \quad i\hbar \frac{\partial}{\partial t} \psi(\mathbf{R}, \theta, t) = \hat{H}(\mathbf{R}, \theta, t) \psi(\mathbf{R}, \theta, t)$$

(on a discretized grid using the split-operator method [3, 13, 14]), starting from an initial wave function $\psi(\mathbf{R}, \theta, t=0)$ taken, in most cases, as the ground (rotationally isotropic) state of the molecule.

2.2. Pendular states. In this high-frequency regime, two different motions are considered: a fast motion associated with the electric field ωt and a slow motion associated with the molecular rotation described by θ . To simplify the presentation, we freeze the molecular internal motions, assuming a rigid rotor behavior. The eigenvectors of the slow motion $\xi_{nJ}(\theta)$ obey, after averaging over the fast motion

within an optical period (and some high-frequency approximations) a Schrödinger equation given by [18]

$$(2.5) \quad \left[\frac{\hbar^2}{2I} j^2 + \frac{\hbar^2}{2I} \frac{M^2}{\sin^2 \theta} + \left(\Delta\alpha + \frac{\mu_0^2}{I\omega^2} \right) \frac{\mathcal{E}_0}{4} \sin^2 \theta + \frac{\Delta\alpha^2 \mathcal{E}_0^4}{256 I \omega^2} \sin^2 2\theta \right] \xi_{nJ}(\theta) = \left(\lambda_n - J\hbar\omega + \frac{\alpha_{\parallel} \mathcal{E}_0^2}{4} \right) \xi_{nJ}(\theta),$$

where $\Delta\alpha = \alpha_{\parallel} - \alpha_{\perp}$. The θ -dependent laser-induced effective potential has a $\sin^2 \theta$ shape and supports the eigenvectors $\xi_{nJ}(\theta)$ which are localized around $\theta = 0$ and π (aligned geometry), in a way which is more marked for increasing intensity. Because of the resulting libration motion for a molecule that is in one of these eigenstates, they are dubbed *pendular states* [15, 29].

It is interesting to note a close analogy with the classical Lagrange equation of the laser-driven rigid rotor under the combined effect of the permanent dipole and the polarizability [12],

$$(2.6) \quad I\ddot{\theta} \simeq \frac{M^2}{I} \frac{\cos \theta}{\sin^3 \theta} - \left(\Delta\alpha + \frac{\mu_0^2}{I\omega^2} \right) \frac{\mathcal{E}_0^2}{4} \sin 2\theta - \frac{\Delta\alpha^2 \mathcal{E}_0^4}{128 I \omega^2} \sin 4\theta.$$

The classical force of the right-hand-side of equation (2.6) is nothing but the gradient of the effective potential of the Hamiltonian version, equation (2.5). This classical analogy leads, upon a change of variable $\Theta = 2\theta$, to the well-known equation of the pendulum,

$$(2.7) \quad \ddot{\Theta} + \Omega^2 \sin \Theta = 0,$$

that librates with small oscillations θ around the laser polarization axis with a frequency

$$(2.8) \quad \Omega = \frac{1}{\sqrt{I}} \left(\frac{1}{2} \frac{\mu_0^2 \mathcal{E}_0^2}{I\omega^2} + \frac{1}{2} \Delta\alpha \mathcal{E}_0^2 \right)^{1/2},$$

where the polarizability remains the leading term as soon as the laser frequency exceeds 315 cm^{-1} (for the HCN molecule), whatever the intensity.

2.3. Control scheme. The question of how to take advantage of the pendular mechanism to control molecular alignment can be answered by referring to adiabatic vs sudden transport dynamics, starting from an initial isotropic distribution ($J = M = 0$, as prepared, for instance, by laser cooling methods [2]).

The adiabatic switching of a laser with rise and fall times of 10 ps (same order as the molecular rotational period) and an intensity of 10^{12} W/cm^2 allows an adiabatic transport on a single (lowest) pendular state with a good alignment during the excitation. Figure 2(a) illustrates the alignment dynamics through the expectation value of $\cos^2 \theta$, i.e.,

$$(2.9) \quad \langle \cos^2 \theta \rangle(t) = \int_0^\pi \cos^2 \theta |\psi(\theta, t)|^2 \sin \theta d\theta.$$

The higher the value, the better the alignment, with $\langle \cos^2 \theta \rangle = 1/3$ corresponding to an isotropic distribution. An alignment of $\langle \cos^2 \theta \rangle \approx 0.64$ is achieved during the pulse but, as expected, the laser extinction adiabatically transports the pendular state back to the isotropic ($J = M = 0$) state.

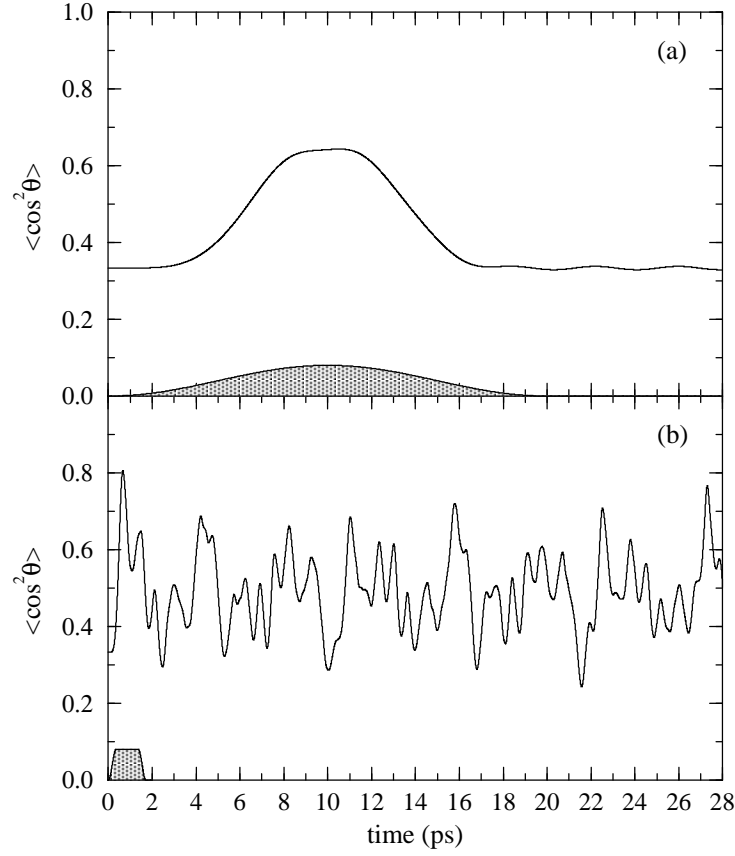


FIGURE 2. Alignment dynamics of the HCN molecule submitted to (a) a long, adiabatic laser pulse of duration 10 ps and intensity 10^{12} W/cm²; (b) a short, sudden pulse of 1.7 ps duration and of intensity 10^{13} W/cm². The pulse envelopes are schematically represented by the shaded areas.

To achieve post-pulse alignment, one may proceed with sudden excitations. Figure 2(b) shows the effect of a sudden pulse of 1.7 ps duration, which excites several pendular states with a specific distribution (for a field frequency resonant with HCN internal vibrations). The particular J distribution reached is such that alignment remains even after the pulse is off, $\langle \cos^2 \theta \rangle(t)$ showing small amplitude oscillations around a value of 0.5.

3. Two-color laser control of orientation (Parity breaking scenarios)

As compared to alignment, orientation, which imposes a given direction, is a more challenging goal that requires symmetry breaking in the forward and backward directions. Two such scenarios are considered in this work. The first concerns the use of two-color pulses, that is a combination of a fundamental frequency ω and its

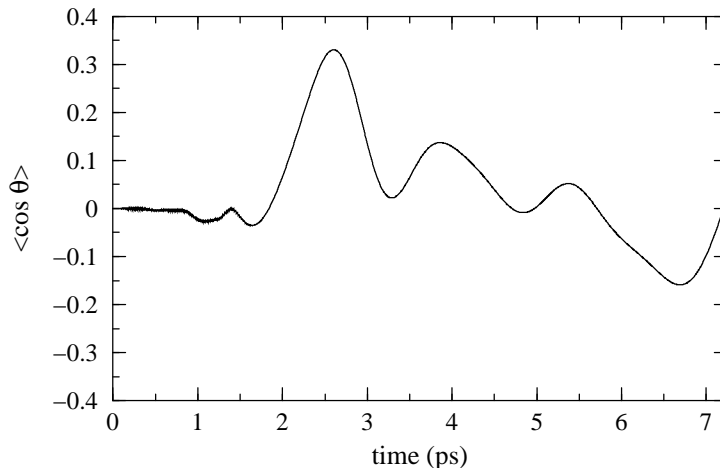


FIGURE 3. Orientation dynamics of the HCN molecule submitted to a laser pulse (1.7 ps duration) combining fields of frequency ω and 2ω , the latter being in resonance with the $v = 0 \rightarrow 1$ vibrational transition of the C–H stretch.

second harmonic 2ω with a resulting field

$$(3.1) \quad \mathcal{E}(t) = \mathcal{E}_0(t) [\cos \omega t + \gamma \cos(2\omega t + \phi)],$$

where maximum asymmetry is reached for $\gamma = 0.5$ and $\phi = 0$. But the asymmetry we are referring to is not in the time dependence of $\mathcal{E}(t)$, which in any case is not enough to produce orientation as, in average over an optical period of the field, the positive and negative contributions are canceling each other. We are rather referring to parity breaking in the rotational quantum numbers J . As opposite to a monochromatic field that excites J 's of the same parity, two-color excitation has the potentiality to mix J 's of different parity. Actually, by taking 2ω in resonance with the $v = 0 \rightarrow 1$ vibrational transition of HCN, the absorption of a single photon 2ω excites odd J 's through the permanent dipole interaction $\mu_0 \mathcal{E}$, whereas the absorption of two photons ω excites even J 's through the polarizability interaction $\alpha \mathcal{E}^2$ (starting from an initial state $J = M = 0$) [8]. It is precisely the mixture of odd and even J 's that produces, by the superposition of associated spherical harmonics, the asymmetrical angular distributions that are looked for. The result is shown in figure 3(a) as the expectation value of $\cos \theta$, which is a measure of orientation (the higher the absolute value, the better the orientation). We see that orientation is actually achieved at the extinction of the laser pulse and more efficiently a short time after the pulse is off, with $\langle \cos \theta \rangle$ reaching 0.3.

Orientation can also be achieved by an adiabatic transport from an initial isotropic state to an asymmetric combination of pendular states by a two-color excitation scheme [16, 17]. Contrary to the result shown in figure 3, such an orientation can only be maintained while the laser is on, similarly to what is observed for alignment in figure 2(a).

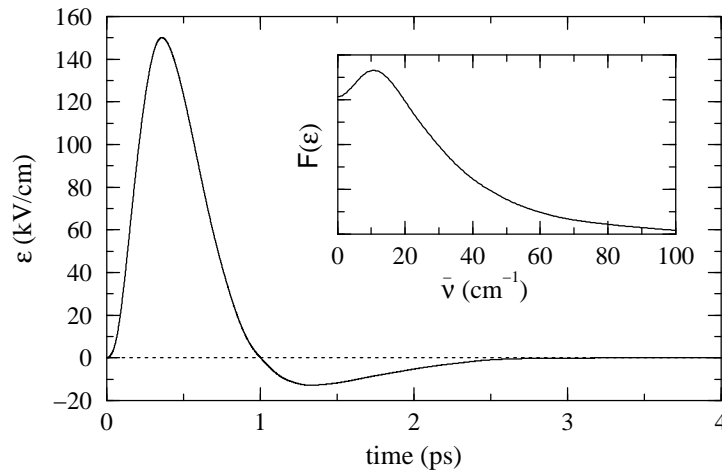


FIGURE 4. Electric field of a half-cycle pulse as a function of time with its Fourier transform given in the inset. (Adapted from reference [28], taken from C. M. Dion, A. Keller, and O. Atabek, *Eur. Phys. J. D* **14** (2001), 249–255, copyright (2001) by EDP Sciences.)

4. Half-cycle pulses and the kick mechanism

The second symmetry breaking scenario addresses the temporal shape of the electric field. The most asymmetrical situation that is experimentally reachable is the use of half-cycle pulses (HCP's) [5]. Such picosecond, far-IR electromagnetic pulses are generated when illuminating a GaAs wafer, in the presence of a pulsed electric field applied across the surface, by a Ti-Sapphire laser [28]. Such pulses have three interesting characteristics (as illustrated on figure 4):

- (i) their intensities remain less than 10^8 W/cm^2 , therefore present no risk of ionization damage on typical diatomic molecules;
- (ii) their relatively broad Fourier transform ($\sim 30 \text{ cm}^{-1}$) shows the presence of non-negligible field components that can induce rotational excitations;
- (iii) they are very sudden with respect to rotation (their positive component lasts typically 1 ps) and very asymmetric (the ratio of the positive to the negative maximum is more than 10).

A direct consequence is that such unipolar pulses can impart a “kick” to the molecule that effectively orients it in the direction of the positive field component, the transfer of angular momentum taking place on the timescale of the short pulse [11]. The long-duration negative tail of the HCP is adiabatic enough not to induce further noticeable changes in the dynamics. Actually, the kick seems the most efficient orientation mechanism up to date. The results are illustrated on the LiCl molecule in terms of the dynamics of the average value of $\cos \theta$, in figure 5.

As in the two-color excitation scenario, the orientation remains modest during the positive part of the pulse, but it develops later and reaches the value $\langle \cos \theta \rangle \sim 0.5$ over a large time period of $\approx 4 \text{ ps}$. The kick mechanism by itself can be evidenced by working out a sudden impact model [11]. Such a model is based on the short duration ($t_p = 1 \text{ ps}$) of the pulse as compared to the molecular rotational

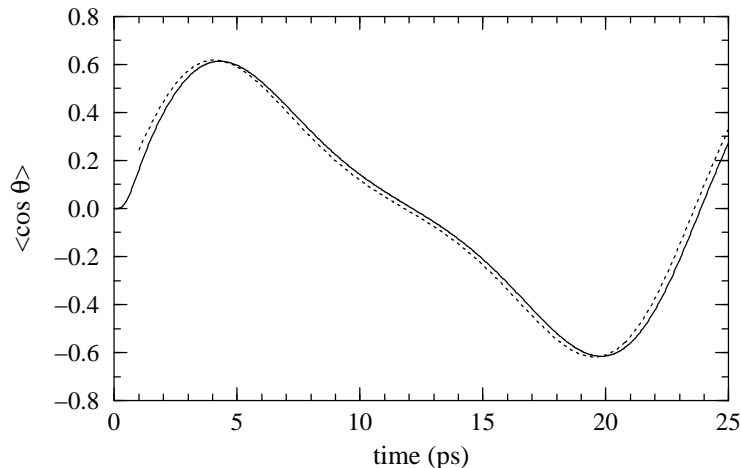


FIGURE 5. Orientation dynamics of the LiCl molecule submitted to the half-cycle pulse of figure 4 (solid line) and using a sudden-impact approximation (dotted line). (Taken from C. M. Dion, A. Keller, and O. Atabek, *Eur. Phys. J. D* **14** (2001), 249–255, copyright (2001) by EDP Sciences.)

period ($T_{\text{rot}} = 24$ ps). The calculation consists in freezing the rotational dynamics during the time the positive part of the HCP is acting. At the lowest order, the approximation is valid as far as

$$(4.1) \quad \frac{B\hat{J}^2 t_p}{\hbar} \sim 0.13J(J+1) \ll 1,$$

where \hat{J} is the rotational kinetic operator and B the rotational constant. The excellent agreement between this sudden impact approximation and the exact time-dependent calculation, with a root-mean-squared difference less than 0.03, eloquently advocates for the kick mechanism.

5. Optimal control scenarios

5.1. General frame. A completely different approach in its philosophy, without a priori reference to any dynamical mechanism, is optimal control. Such a scheme presents a general structure resting on three steps:

- (i) an evaluation function, $\langle \cos \theta \rangle(t)$, involving the numerical solution of the time-dependent Schrödinger equation (using split operator [3, 13, 14] or basis expansion [4] techniques). For a laser-driven rigid rotor this amounts to solving

$$(5.1) \quad i\hbar \frac{\partial}{\partial t} \psi(\theta, \varphi, t) = \hat{H}(t) \psi(\theta, \varphi, t)$$

with

$$(5.2) \quad \hat{H}(t) = B\hat{J}^2 - \mu_0 \mathcal{E}(t) \cos \theta - [(\alpha_{\parallel} - \alpha_{\perp}) \cos^2 \theta + \alpha_{\perp}] \frac{\mathcal{E}^2(t)}{2}$$

in order to calculate

$$(5.3) \quad \langle \cos \theta \rangle(t) = \int_0^{2\pi} \int_0^\pi |\psi(\theta, \varphi; t)|^2 \cos \theta \sin \theta d\theta d\varphi$$

- (ii) a set of parameters defining the temporal shape of the laser pulse, given here as a superposition of individual sine-square functions with intermediate plateau values,

$$(5.4) \quad \mathcal{E}(t) = \sum_{n=1}^N \mathcal{E}_n(t) \sin(\omega_n t + \phi_n)$$

with

$$(5.5) \quad \mathcal{E}_n(t) = \begin{cases} 0 & \text{if } t \leq t_{n0} \\ \mathcal{E}_{n0} \sin^2 \left[\frac{\pi}{2} \left(\frac{t-t_{n0}}{t_{n1}-t_{n0}} \right) \right] & \text{if } t_{n0} \leq t \leq t_{n1} \\ \mathcal{E}_{n0} & \text{if } t_{n1} \leq t \leq t_{n2} \\ \mathcal{E}_{n0} \sin^2 \left[\frac{\pi}{2} \left(\frac{t_{n3}-t}{t_{n3}-t_{n2}} \right) \right] & \text{if } t_{n2} \leq t \leq t_{n3} \\ 0 & \text{if } t \geq t_{n3} \end{cases}$$

- (iii) a target j , i.e., an optimization criterion.

The optimization aims at the obtainment of the laser parameters (intensity, frequency, temporal shape defined by rise and fall times, together with possible plateau durations) that optimally satisfy the target j . The optimization procedure we use is based on genetic algorithms [1, 22] operating in a $7N$ dimensional parameter space (i.e., 7 parameters for each of the N individual pulses). It is worthwhile noting that a given criterion puts the emphasis on a specific feature of the orientation, such that different criteria may lead to quite different results. This is basically related to the fact that orientation can by no way be achieved by monitoring a single quantum state or a unique and pre-determined superposition of states. We will analyze in some detail the consequences of the choice of specific criteria. But before doing this, let us proceed to a first optimization retaining an intuitive, simple criterion that consists in the maximization of $\langle \cos \theta \rangle$ for a single time t_f when the laser field is off,

$$(5.6) \quad j = |\langle \cos \theta \rangle(t_f)|.$$

5.2. The kicked molecule. The optimal electric field which is obtained and illustrated in figure 6(a) turns out to be one of the most enlightening results of this study. A combination of three individual pulses (i.e., 21 parameters to be optimized) leads to a very sudden and asymmetric pulse, followed by a null plateau and some rather symmetrical oscillations. The molecule (HCN taken as a rigid rotor, in this example) orients through the already discussed kick mechanism due to the fast angular momentum transfer by the unipolar pulse at about $t = 0.3$ ps and during the null plateau lasting 1 ps. The symmetrical oscillations of this field between 1 and 1.7 ps do not seem to play a major part in this dynamics. Here again, the kick mechanism can be evidenced by a sudden impact approximation which closely follows the $\langle \cos \theta \rangle$ dynamics at least until 1.5 ps [see figure 6(b)]. It is important to note that an accuracy of 4 digits in the genetic algorithm is achieved for the intensities, frequencies, and absolute phase differences in order to produce the particular shape of the electric field of figure 6(a), responsible of the subsequent kick mechanism. Figure 7 accounts for the long-time dynamics (i.e., for

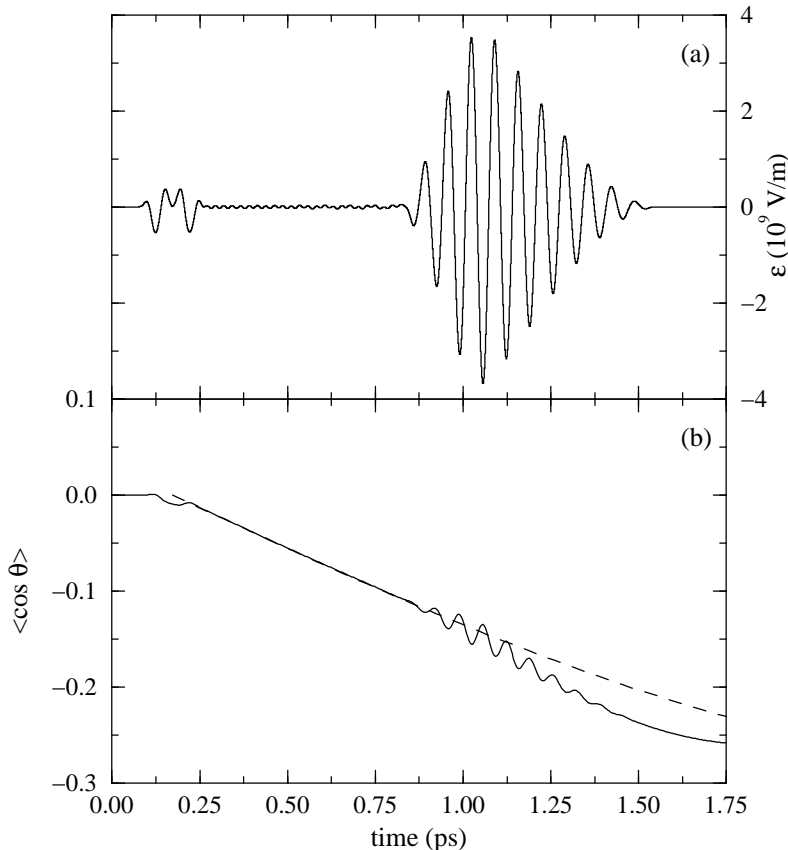


FIGURE 6. (a) Laser field resulting from the optimization using criterion $j = |\langle \cos \theta \rangle(t_f)|$, for the HCN molecule in a rigid-rotor model. (b) Orientation dynamics obtained using this field (solid line) and using a sudden-impact approximation (dashed line). (Taken from C. M. Dion, A. Ben Haj-Yedder, E. Cancès, C. Le Bris, A. Keller, and O. Atabek, *Phys. Rev. A* **65** (2002), 063408, copyright (2002) by the American Physical Society.)

full rotational period). Maximum orientation is reached at about $t \approx 10$ ps and lasts for about 3 ps. It is interesting to note that the result of the sudden impact model based on the first kick (at ~ 0.5 ps) can further be improved by introducing the effect of the oscillatory field acting after the null plateau as a second kick (that is again freezing the rotational motion during the time over which the molecule experiences this second interaction).

An analysis of the optimized laser pulse obtained can be carried out using the short-time Fourier transform of the electric field, given by

$$(5.7) \quad \mathcal{F}(\omega, t) = \int_{-\infty}^{+\infty} \mathcal{E}(\tau) f_w(\tau - t) e^{-i\omega\tau} d\tau,$$

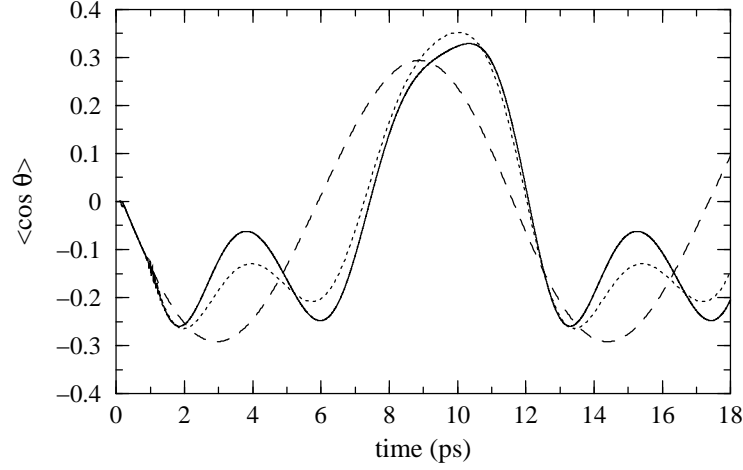


FIGURE 7. Same orientation dynamics as figure 6(b), but given for an entire rotational period of the HCN molecule ($T_{\text{rot}} = 11.45$ ps) and with an additional curve (dotted line) corresponding to the sudden-impact approximation with two kicks (see text). (Taken from C. M. Dion, A. Ben Haj-Yedder, E. Cancès, C. Le Bris, A. Keller, and O. Atabek, *Phys. Rev. A* **65** (2002), 063408, copyright (2002) by the American Physical Society.)

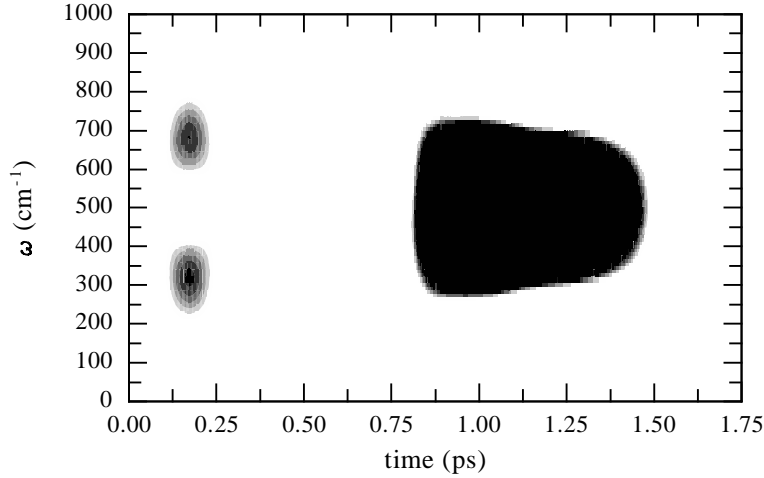


FIGURE 8. Short-time Fourier transform [equation (5.7)] of the field given in figure 6(a).

with f_w a windowing function (we have taken a Tukey-Hanning window [21] of total width 0.29 ps). The result is shown in figure 8 as a 2D representation of the electric field amplitude as a function of ω and t . The asymmetric feature present in the field at around ~ 0.15 ps turns out to be the superposition of two components at frequencies ω and 2ω . This corresponds to the most asymmetrical electric field

which, when truncated at a time that is not an integer of the optical period, leads to a non-zero field integral imparting the kick to the molecule. This is followed later on by a component centered around a single frequency which also leads to a second, smaller kick. Such a result has a broader applicability: the same pulse applied to a different molecule (e.g., LiF) produces similar orientation dynamics [9].

5.3. The optimization criteria. We now return to a thorough analysis of the consequences of choosing different criteria in the optimization scheme. Ideally, the best orientation is the one which is the most efficient (i.e., with a value of $\langle \cos \theta \rangle$ close to one) and which lasts forever. The relative merits of the different criteria can thus be quantitatively measured in terms of the efficiency and the duration of the orientation. All calculations that are presented hereafter apply to the LiF molecule and are conducted within a parameter sampling space limited to frequencies comprised in between 500 and 4000 cm^{-1} , to individual pulses extinction times less than t_f taken as one tenth of a rotational period (as we are seeking post-pulse orientation resulting from a sudden excitation, which also helps in keeping calculations within acceptable CPU times) and to laser intensities not exceeding $3 \times 10^{13} \text{ W/cm}^2$ (to avoid risk of ionization damage, having in mind that $1.1 \times 10^{14} \text{ W/cm}^2$ is the predicted first ionization threshold for LiF).

The criteria can roughly be classified into two groups: simple, when they emphasize either efficiency or duration; hybrid, when they realize a compromise between efficiency and duration. Aiming at the best orientation efficiency, a more flexible criterion than the one that has been used so far [equation (5.6)] is

$$(5.8) \quad j_1 \equiv \max_{t \in [t_f, t_f + T_{\text{rot}}]} |\langle \cos \theta \rangle(t)|,$$

the maximum being now taken at any time within the interval $[t_f, t_f + T_{\text{rot}}]$ (taking into account the periodical behavior of the orientation dynamics with respect to the rotational period T_{rot}). The result is displayed in figure 9. The electric field thus obtained is built up from two individual pulses of comparable intensities, with frequencies in a ratio of 2 responsible for the double wiggles in the amplitude, as illustrated in figure 10. Excellent orientation ($\langle \cos \theta \rangle \approx -0.8$) is achieved with a time delay of about 6 ps after the pulse is off. This molecular response time to the laser interaction is the time needed for the specific phase interferences to occur in the rotational wave packet. Such occurrences of the field-free dynamics are periodical (molecular rotational periodicity T_{rot}), give rise to the revival structures discussed in the literature [25], and are common to all results presented hereafter.

The criterion j_1 fails in producing long-lasting orientation (the time interval over which $|\langle \cos \theta \rangle|$ remains larger than 70% of its maximum value does not exceed 0.37 ps). Another criterion is built to precisely maximize the orientation duration τ ,

$$(5.9) \quad j_2 \equiv \max_{t \in [t_f, t_f + T_{\text{rot}}]} \frac{\tau}{T_{\text{rot}}},$$

where τ is defined as the time over which an orientation exceeding $j_1/\sqrt{2}$ is kept,

$$(5.10) \quad \frac{j_1}{\sqrt{2}} \leq |\langle \cos \theta \rangle(t)| \leq j_1.$$

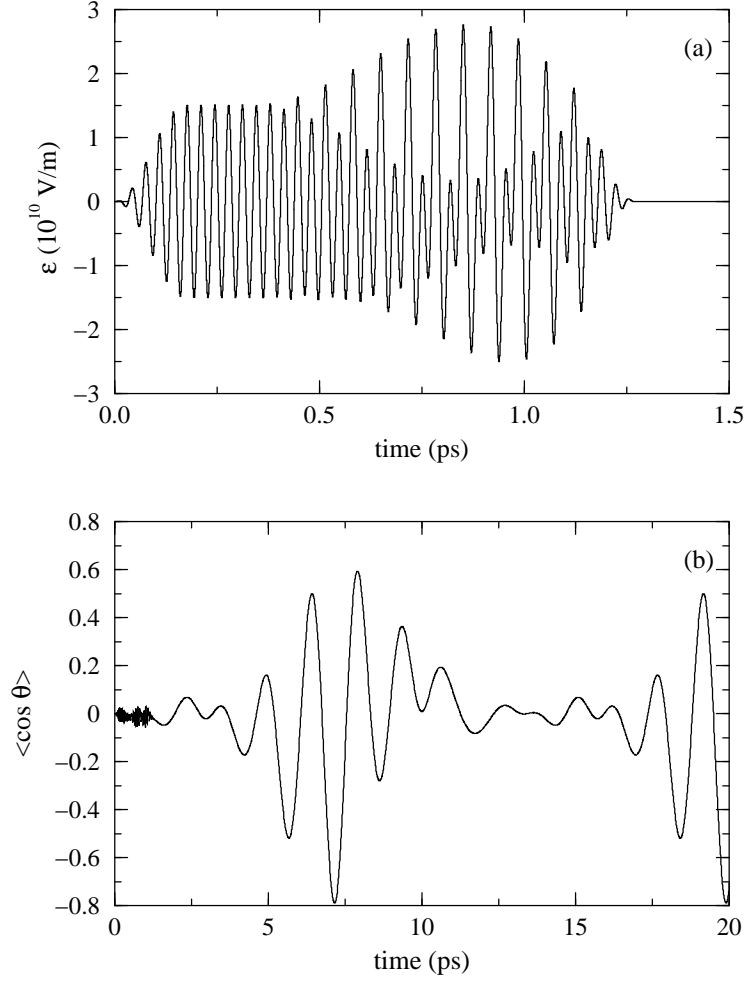


FIGURE 9. (a) Laser field resulting from the optimization using criterion $j_1 = \max_{t \in [t_f, t_f + T_{\text{rot}}]} |\langle \cos \theta \rangle(t)|$, for the LiF molecule in a rigid-rotor model. (b) Corresponding orientation dynamics. (Adapted from A. Ben Haj-Yedder, A. Auger, C. M. Dion, E. Cancès, A. Keller, C. Le Bris, and O. Atabek, Phys. Rev. A **66** (2002), 063401, copyright (2002) by the American Physical Society.)

The optimized electric field shows two intense, sudden, high frequency and well separated components (see figure 11), inducing a smooth behavior for $\langle \cos \theta \rangle(t)$ as expected for large values of τ , but unfortunately the orientation is very inefficient.

The weakness of these simple criteria may be overcome by building physically more sound hybrid criteria that combine the advantages of the previous requirements for a better compromise between efficiency and duration. Our best result is obtained with a criterion that maximizes a functional of $\langle \cos \theta \rangle^2(t)$ over an entire

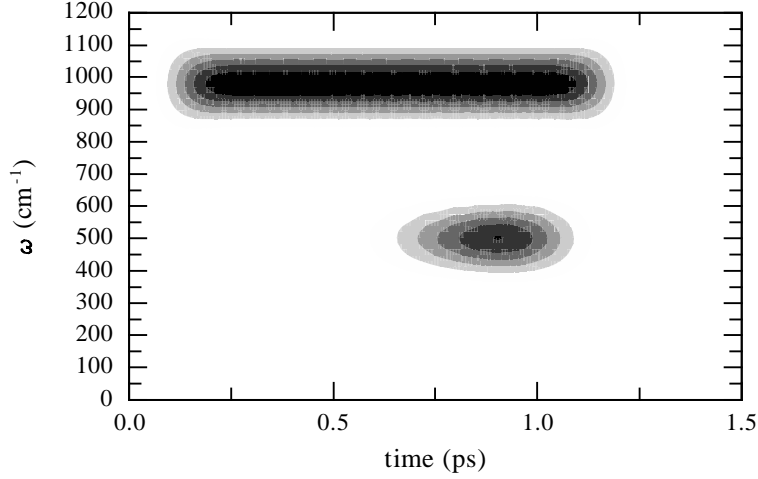


FIGURE 10. Short-time Fourier transform [equation (5.7)] of the field given in figure 9(a).

rotational period,

$$(5.11) \quad j_3 \equiv \max \frac{1}{T_{\text{rot}}} \int_{t_f}^{t_f + T_{\text{rot}}} \mathcal{C}^2(t) dt,$$

where $\mathcal{C}(t)$ is tailored as to put the emphasis on time intervals where $\langle \cos \theta \rangle$ is larger than some fixed value (0.4 in our case) through an appropriate weighting factor (0.1 in our case):

$$(5.12) \quad \mathcal{C}(t) = \begin{cases} 0.1 \langle \cos \theta \rangle(t) & \text{if } \langle \cos \theta \rangle(t) < 0.4 \\ \langle \cos \theta \rangle(t) & \text{elsewhere} \end{cases}$$

Figure 12 displays the optimized field built up from two sudden, intense pulses, with very close frequencies (742 cm^{-1} and 808 cm^{-1}) giving a beat-like structure. It is worthwhile noting that the resulting field appears as two beats of similar frequency $\sim 780 \text{ cm}^{-1}$ (see figure 13), but we failed in analyzing them in terms of a double kick mechanism (the sudden impact model not providing the expected orientation dynamics). Finally, in terms of quantitative measurements, this field achieves orientation which lasts for 0.7 ps with a $|\langle \cos \theta \rangle|$ larger than 0.5, and is one of the best results of the literature.

5.4. Robustness with respect to temperature. All calculations so far presented concern an initially rotationless molecule, $J = M = 0$, M being the quantum number labelling the projection of the rotational angular momentum on the laser polarization vector taken as the laboratory reference axis. With respect to experimental conditions, such a situation concerns a molecule at a temperature of $T = 0 \text{ K}$. Starting from such a state (prepared by laser cooling methods, for instance [2]), linearly polarized photon absorption only populate higher J levels; M , being a good quantum number (labelling an azimuthal angular motion, well separated due to cylindrical symmetry), remains unchanged (i.e., zero). Increasing temperature, on the other hand, populates higher J levels with all their M components, $|M| = 0, 1, \dots, J$, within a Boltzmann distribution. For a given component,

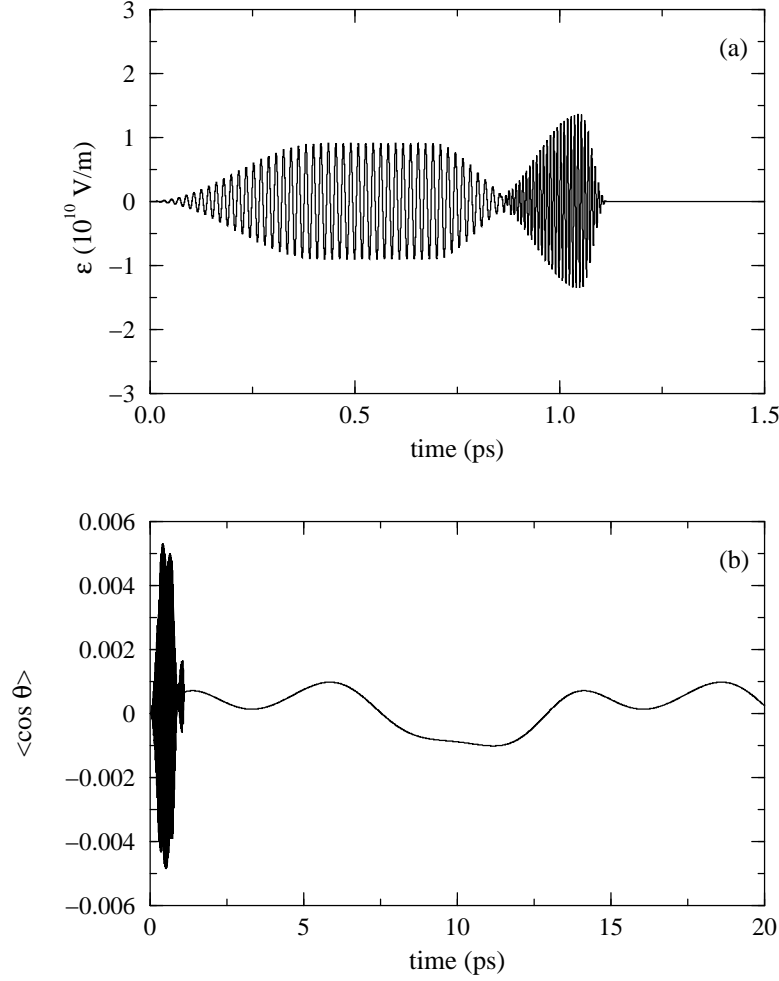


FIGURE 11. (a) Laser field resulting from the optimization using criterion $j_2 = \max_{t \in [t_f, t_f + T_{\text{rot}}]} \tau / T_{\text{rot}}$, for the LiF molecule in a rigid-rotor model. (b) Corresponding orientation dynamics. (Adapted from A. Ben Haj-Yedder, A. Auger, C. M. Dion, E. Cancès, A. Keller, C. Le Bris, and O. Atabek, Phys. Rev. A **66** (2002), 063401, copyright (2002) by the American Physical Society.)

a vectorial representation of the field-driven classical rigid rotor leads to

$$(5.13) \quad \sin \theta = \frac{|M|}{J},$$

the total angular momentum vector \mathbf{J} being orthogonal to the rigid rotor axis \mathbf{R} and θ being the polar angle positioning \mathbf{R} with respect to the laser polarization vector. Large values of M would thus prevent alignment and orientation, θ reaching a value as high as $\pi/2$ for $|M| = J$, as illustrated in figure 14. Using linearly polarized laser

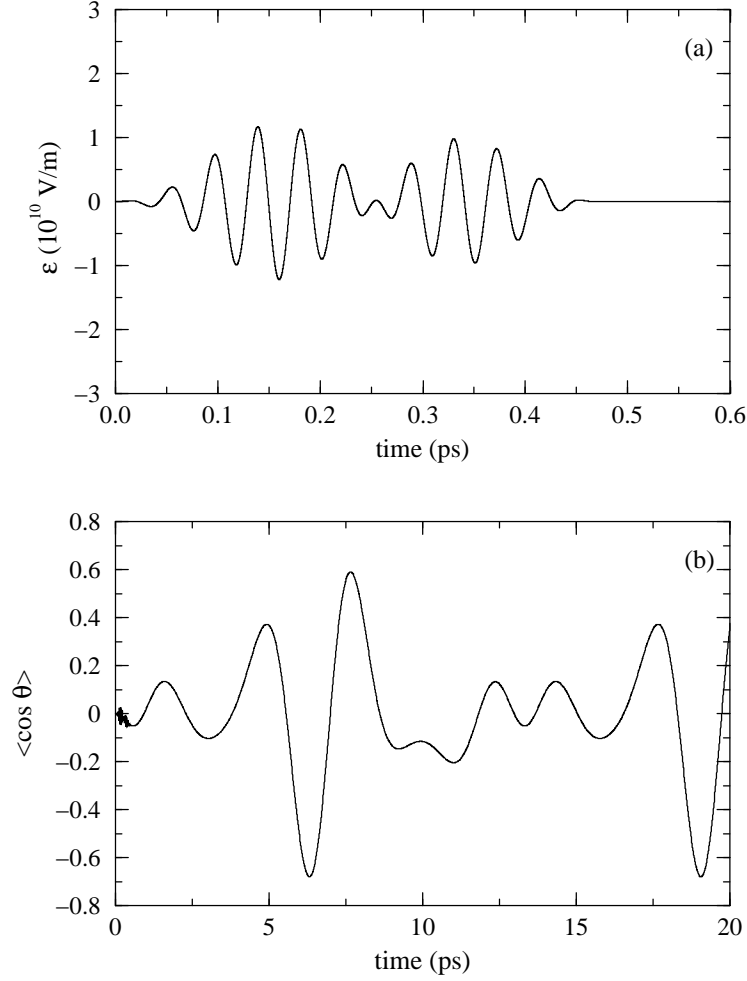


FIGURE 12. (a) Laser field resulting from the optimization using criterion $j_3 = \max(1/T_{\text{rot}}) \int_{t_f}^{t_f+T_{\text{rot}}} \mathcal{C}^2(t) dt$, for the LiF molecule in a rigid-rotor model. (b) Corresponding orientation dynamics. (Adapted from A. Ben Haj-Yedder, A. Auger, C. M. Dion, E. Cancès, A. Keller, C. Le Bris, and O. Atabek, Phys. Rev. A **66** (2002), 063401, copyright (2002) by the American Physical Society.)

sources, no reduction of M could be achieved, showing that orientation is no more a mathematically controllable process at non-zero temperature. Because they are breaking the overall cylindrical symmetry, elliptically polarized lasers are possible tools for modifying the values of M , in an optimally controlled way to lead again to alignment and orientation. Work in this direction is now undertaken in our group.

It remains however that the robustness of our optimal control scheme can be checked at least for some low temperatures. Instead of our previous evaluation function (5.3), we have to refer to a temperature dependent Boltzmann averaging

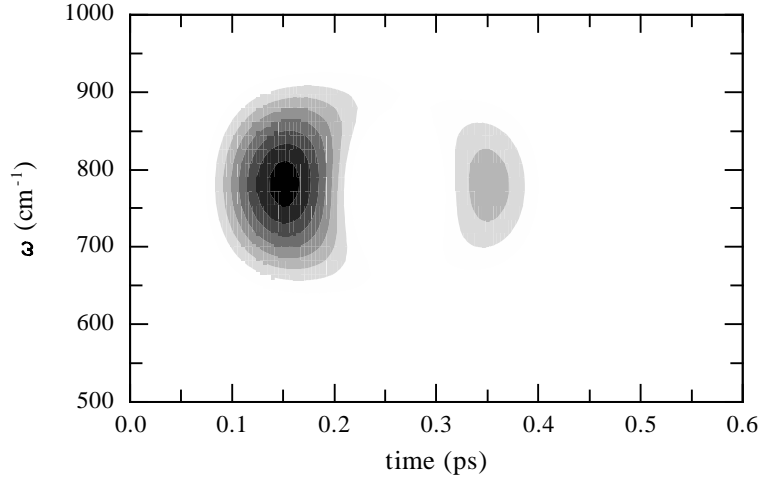


FIGURE 13. Short-time Fourier transform [equation (5.7)] of the field given in figure 12(a).

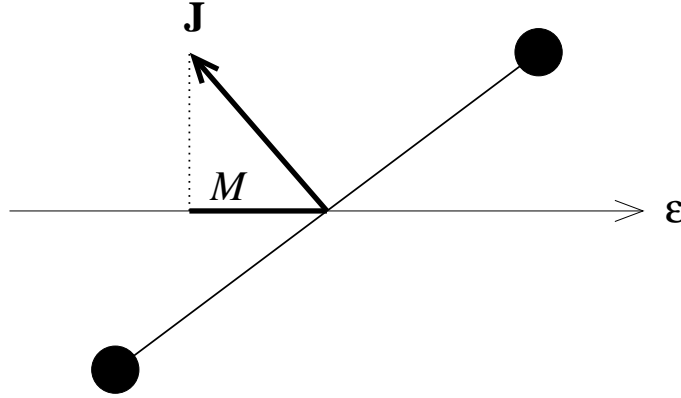


FIGURE 14. Schematic representation of the total angular momentum vector \mathbf{J} and its projection M on the laser polarization axis \mathcal{E} , for a (diatomic) linear molecule. By definition, \mathbf{J} is perpendicular to the internuclear axis, therefore if $|M| = J$ the molecule is perpendicular to the laser polarization axis.

of $\cos \theta$,

$$(5.14) \quad \langle \langle \cos \theta \rangle \rangle (t) = Q^{-1} \sum_J^{J_{\max}} \exp \left[\frac{-BJ(J+1)}{k_B T} \right] \sum_{M=-J}^J \langle \cos \theta \rangle_{J,M} (t),$$

where $\langle \cos \theta \rangle_{J,M} (t)$ results from the dynamics of an individual initial state J, M included in a summation over J and M with its appropriate exponential weighting factor, and a partition function

$$(5.15) \quad Q = \sum_J^{J_{\max}} (2J+1) \exp \left[\frac{-BJ(J+1)}{k_B T} \right],$$

for normalization.

Figure 15 presents the results for the LiF molecule at $T = 5$ K. Here again, simple (j_1) and hybrid (j_3 -like) criteria are referred to. The dotted line (panel a) represents the orientation dynamics at 5 K [equation (5.14)] but with the electric field of figure 9(a) optimized for $T = 0$ K. This is, precisely, to show how orientation effects are rapidly washed out when incorporating higher initial M 's. A field optimized for $T = 5$ K restitutes again the oscillatory structures of $\langle\langle\cos\theta\rangle\rangle(t)$, with however reduced amplitudes (solid line of panel a). A more satisfactory result requires the introduction of an additional individual pulse bringing 21 free parameters in the optimization scheme. The result is given in figure 9(b) with an orientation higher than $\langle\langle\cos\theta\rangle\rangle = 0.27$ kept over a time of about 0.25 ps. The result of the hybrid criterion j_3 with a 21-free-parameters optimization is illustrated in figure 9(c). A much longer time duration (~ 0.4 ps) is achieved for about the same efficiency.

6. Conclusion

The complementarity between basic mechanisms and optimal control schemes can be summarized either by referring to the way of implementing mechanisms in control, or reversely of identifying mechanisms revealed from control.

The first strategy rests on three observations:

- (i) there is no single solution arising from optimal control scenarios (not only different criteria, but also different sampling spaces for parameters would lead to different results);
- (ii) a careful study of the laser-induced dynamics can help to the identification (or guess) of some basic mechanisms leading to the desired observable;
- (iii) by appropriately building the targets and delineating the parameter sampling space, we can help the optimal control scheme to take advantage of the mechanisms.

The second strategy consists in learning a dynamical mechanism presenting some robustness from the optimal control results. This mechanism may be used directly for reaching the desired observable (strategy 2) or further improved by implementing it again in a control scenario with some additional flexibility (strategy 1).

The kick mechanism and the optimal control carried out using sudden pulses is an example that illustrates these two routes. The mechanism has actually been depicted using half-cycle pulses and a sudden impact model. The parameter sampling space for the optimal control, although not constrained, has been limited to sudden pulses that are precisely compatible with the kick mechanism. This control scenario has finally revealed a double-kick mechanism which can serve as a starting point of a train of kicks, that we can merely guess to provide even better orientation. Finally, this mechanism, together with some additional free parameters such as the time delay between the successive kicks, can be re-injected (re-introduced) in an optimal control scheme (strategy 1) aiming at improving its efficiency. We are presently pursuing some investigations in this direction.

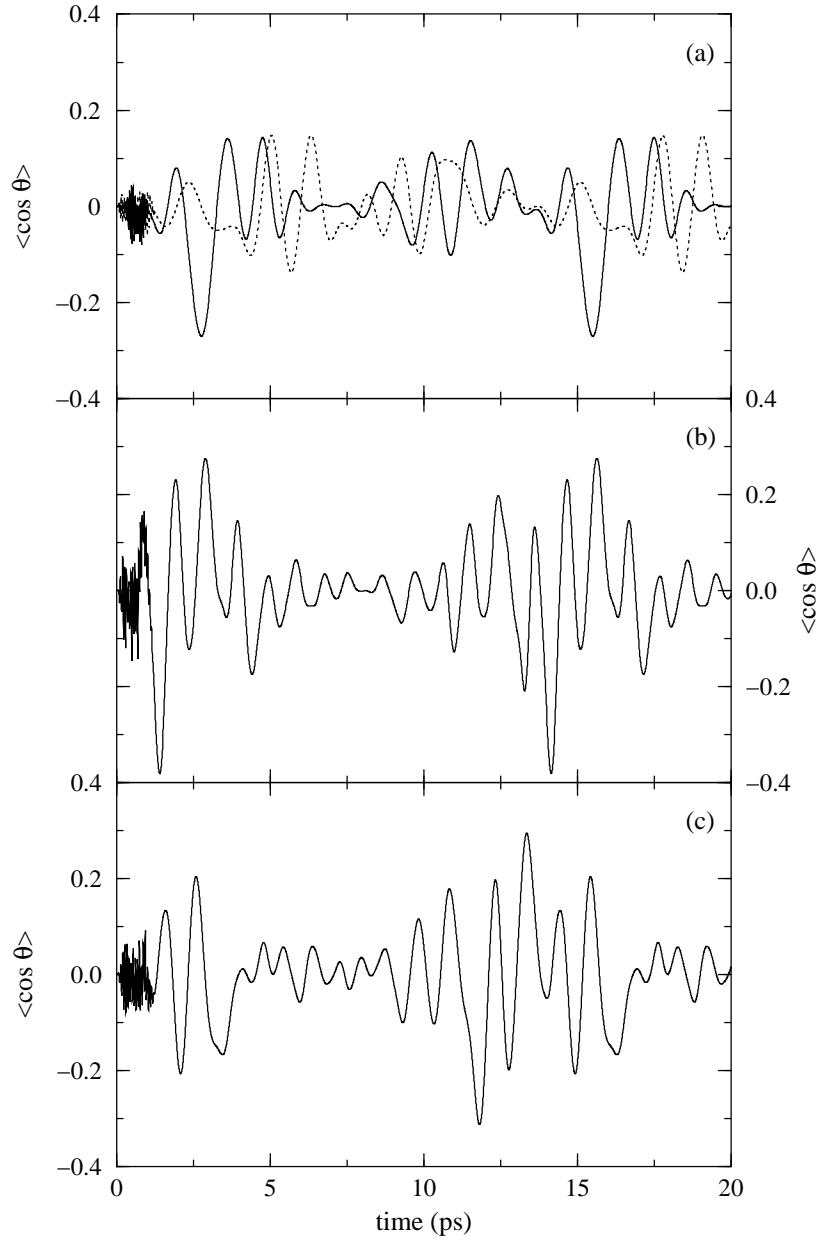


FIGURE 15. Effect of temperature on the orientation dynamics of the LiF molecule. (a) Dotted line: using the laser field obtained from a $T = 0$ K optimization with criterion j_1 [see figure 9(a)], but applied to an initial distribution of molecules at $T = 5$ K. Solid line: using the laser field obtained from a $T = 5$ K optimization with criterion j_1 . (b) Same as (a), but using a superposition of 3 laser pulses. (c) Same as (b), but using criterion j_3 . (Adapted from A. Ben Haj-Yedder, A. Auger, C. M. Dion, E. Cancès, A. Keller, C. Le Bris, and O. Atabek, Phys. Rev. A **66** (2002), 063401, copyright (2002) by the American Physical Society.)

References

- [1] A. Auger, A. Ben Haj-Yedder, E. Cancès, C. Le Bris, C. M. Dion, A. Keller, and O. Atabek, *Optimal laser control of molecular systems: Methodology and results*, Math. Models Methods Appl. Sci. **12** (2002), 1281–1315.
- [2] J. T. Bahns, P. L. Gould, and W. C. Stwalley, *Formation of cold ($T \leq 1$ K) molecules*, Adv. At. Mol. Opt. Phys. **42** (2000), 171–224.
- [3] A. D. Bandrauk and H. Shen, *Improved exponential split operator method for solving the time-dependent Schrödinger equation*, Chem. Phys. Lett. **176** (1991), 428–432.
- [4] A. Ben Haj-Yedder, A. Auger, C. M. Dion, E. Cancès, A. Keller, C. Le Bris, and O. Atabek, *Numerical optimization of laser fields to control molecular orientation*, Phys. Rev. A **66** (2002), 063401.
- [5] P. Bucksbaum, *Wave packets and half-cycle pulses*, The Physics and Chemistry of Wave Packets (J. A. Yeazell and T. Uzer, eds.), Wiley, New York, 2000.
- [6] E. Charron, A. Giusti-Suzor, and F. H. Mies, *Fragment angular distribution in one- and two-color photodissociation by strong laser fields*, Phys. Rev. A **49** (1994), R641–R644.
- [7] B. K. Dey, M. Shapiro, and P. Brumer, *Coherently controlled nanoscale molecular deposition*, Phys. Rev. Lett. **85** (2000), 3125–3128.
- [8] C. M. Dion, A. D. Bandrauk, O. Atabek, A. Keller, H. Umeda, and Y. Fujimura, *Two-frequency IR laser orientation of polar molecules. Numerical simulations for HCN*, Chem. Phys. Lett. **302** (1999), 215–223.
- [9] C. M. Dion, A. Ben Haj-Yedder, E. Cancès, C. Le Bris, A. Keller, and O. Atabek, *Optimal laser control of orientation: The kicked molecule*, Phys. Rev. A **65** (2002), 063408.
- [10] C. M. Dion, S. Chelkowski, A. D. Bandrauk, H. Umeda, and Y. Fujimura, *Numerical simulation of the isomerization of HCN by two perpendicular intense IR laser pulses*, J. Chem. Phys. **105** (1996), 9083–9092.
- [11] C. M. Dion, A. Keller, and O. Atabek, *Orienting molecules using half-cycle pulses*, Eur. Phys. J. D **14** (2001), 249–255.
- [12] C. M. Dion, A. Keller, O. Atabek, and A. D. Bandrauk, *Laser-induced alignment dynamics of HCN: Roles of the permanent dipole moment and the polarizability*, Phys. Rev. A **59** (1999), 1382–1391.
- [13] M. D. Feit, J. A. Fleck, Jr., and A. Steiger, *Solution of the Schrödinger equation by a spectral method*, J. Comput. Phys. **47** (1982), 412–433.
- [14] J. A. Fleck Jr., J. R. Morris, and M. D. Feit, *Time-dependent propagation of high energy laser beams through the atmosphere*, Appl. Phys. **10** (1976), 129–160.
- [15] B. Friedrich and D. Herschbach, *Alignment and trapping of molecules in intense laser fields*, Phys. Rev. Lett. **74** (1995), 4623–4626.
- [16] S. Guérin, L. P. Yatsenko, H. R. Jauslin, O. Faucher, and B. Lavorel, *Orientation of polar molecules by laser induced adiabatic passage*, Phys. Rev. Lett. **88** (2002), 233601.
- [17] T. Kanai and H. Sakai, *Numerical simulations of molecular orientation using strong, non-resonant, two-color laser fields*, J. Chem. Phys. **115** (2001), 5492–5497.
- [18] A. Keller, C. M. Dion, and O. Atabek, *Laser-induced molecular rotational dynamics: A high-frequency Floquet treatment*, Phys. Rev. A **61** (2000), 023409.
- [19] V. Kurkal and S. A. Rice, *Sequential STIRAP-based control of the HCN→CNH isomerization*, Chem. Phys. Lett. **344** (2001), 125–137.
- [20] M. D. Poulsen, E. Skovsen, and H. Stapelfeldt, *Photodissociation of laser aligned iodobenzene: Towards selective photoexcitation*, J. Chem. Phys. **117** (2002), 2097–2102.
- [21] M. B. Priestley, *Spectral analysis and time series*, Academic Press, San Diego, 1981.
- [22] M. Schoenauer, A. Auger, and A. Ben haj Yedder, *Overview and software guide of evolutionary algorithms; Case study in quantum control*, CRM Proc. Lecture Notes (this issue).
- [23] T. Seideman, *Manipulating external degrees of freedom with intense light: Laser focusing and trapping of molecules*, J. Chem. Phys. **106** (1997), 2881–2892.
- [24] ———, *Molecular optics in an intense laser field: A route to nanoscale design*, Phys. Rev. A **56** (1997), R17–R20.
- [25] ———, *Revival structure of aligned rotational wave packets*, Phys. Rev. Lett. **83** (1999), 4971–4974.
- [26] H. Stapelfeldt, H. Sakai, E. Constant, and P. B. Corkum, *Deflection of neutral molecules using the nonresonant dipole force*, Phys. Rev. Lett. **79** (1997), 2787–2790.

- [27] M. G. Tenner, E. W. Kuipers, A. W. Kleyn, and S. Stolte, *Direct inelastic scattering of oriented NO from Ag(111) and Pt(111)*, J. Chem. Phys. **94** (1991), 5197–5207.
- [28] D. You, R. R. Jones, P. H. Bucksbaum, and D. R. Dykaar, *Generation of high-power sub-single-cycle 500-fs electromagnetic pulses*, Opt. Lett. **18** (1993), 290–292.
- [29] B. A. Zon and B. G. Katsnel’son, *Nonresonant scattering of intense light by a molecule*, Sov. Phys. JETP **42** (1975), 595–601.

LABORATOIRE DE PHOTOPHYSIQUE MOLÉCULAIRE DU CNRS, BÂTIMENT 213, UNIVERSITÉ PARIS-SUD, 91405 ORSAY, FRANCE

E-mail address: `osman.atabek@ppm.u-psud.fr`

CERMICS, ÉCOLE NATIONALE DES PONTS ET CHAUSSÉES, CITÉ DESCARTES, CHAMPS-SUR-MARNE, 77455 MARNE-LA-VALLÉE, FRANCE

E-mail address: `claudio.dion@physics.org`